Nonlinear Analysis: Modelling and Control, Online First, 1–24
https://doi.org/10.15388/namc.2023.28.32845

Vilnius University Press

Spatiotemporal dynamics in a toxin-producing predator–prey model with threshold harvesting*

Luhong Ye[a,b], **Hongyong Zhao**[a,1], **Daiyong Wu**[b]

[a]School of Mathematics,
Nanjing University of Aeronautics and Astronautics,
Nanjing 210016, China
hyzho1967@126.com

[b]Department of Mathematics and Physical Sciences,
Anqing Normal University,
Anqing 246133, China

Received: May 13, 2022 / **Revised:** July 5, 2023 / **Published online:** July 27, 2023

Abstract. In this paper, we propose a toxin-producing predator–prey model with threshold harvesting and study spatiotemporal dynamics of the model under the homogeneous Neumann boundary conditions. At first, the persistence property of solutions to the system is investigated. Then the explicit requirements for the existence of nonconstant steady state solutions are derived by studying the relevant characteristic equation. These steady states occur from related constant steady states via steady state bifurcation. Throughout the analysis of the amplitude equations of Turing pattern by the multiple scale method, pattern formation can be found. Finally, we display numerical simulations to verify the theoretical outcomes.

Keywords: Turning instability, bifurcation, nonconstant steady state, toxicity, threshold harvesting.

1 Introduction

Environmental protection and ecologically sustainable development have always been our concerns. However, in recent years, there have been a lot of take-outs and express deliveries around us. They do bring convenience to our life. But at the same time, they cause a lot of rubbish in the city and pollute the environment [1, 12]. In addition, a variety of chemicals and industrial waste gas will also release many toxic substances, which directly affect human health. He et al. [6] studied the impact of atmosphere pollution on the risk of respiratory infection. They also pollute water, land, and air [13, 28], and

*This research was is partially supported by the Key Project of the Natural Science Foundation of China (grant No. 11971013), the Natural Science Research of Anhui Higher Education Institutions of China (grant Nos. KJ2020A0492 and KJ2020A0491), the Natural Science Foundation of Anhui Province of China (grant No. 2108085MA10).

[1]Corresponding author.

indirectly lead to the species extinction. The effects of pollutants on a single-species population were discussed, and some sufficient requirements were obtained to guarantee the endurance of the population in [27]. So it is necessary to study the impact of toxic substances.

At present, some literatures, such as [3, 4, 8, 11, 14, 16–19, 22–26], have studied the effects of toxins on different ecosystem species. [4] indicated that once some external toxic substances directly infected the prey, then the predator consuming polluted prey was indirectly influenced by the toxicant. So we use $\theta_1 u^3$ to mark the infection of the prey by some external toxicant, and $\theta_2 v^2$ to signify the infection of the predator by this infected prey for food. Because of $\mathrm{d}(\theta_1 u^3)/\mathrm{d}u = 3\theta_1 u^2 > 0$, $\mathrm{d}(\theta_2 v^2)/\mathrm{d}v = 2\theta_2 v > 0$, the toxicant growth is accelerated with more prey eating such polluted food. It is analogical to the predator. As $0 < \theta_2 < \theta_1 < 1$, so the toxicant has less effect on the predator than on the prey.

Most predator–prey models with harvesting only considered constant, linear, or nonlinear functions such as fishery harvesting [28] and [1, 2, 7, 9, 10]. However, it is not very realistic as pointed out by Rebaza [21]. Based on the above analysis, the harvesting is assumed proportional to the prey density after the prey gets to the threshold because the facilities for harvesting or resource protection are limited. It keeps constant after the population density reaches T.

We present the toxin-producing predator–prey model with threshold harvesting:

$$\begin{aligned}
&\frac{\partial u}{\partial t} = d_1 \Delta u + ru\left(1 - \frac{u}{K}\right) - muv - H(u) - \theta_1 u^3, \quad (x,t) \in \Omega \times (0,+\infty),\\
&\frac{\partial v}{\partial t} = d_2 \Delta v + cmuv - \eta v - \theta_2 v^2, \quad (x,t) \in \Omega \times (0,+\infty),\\
&\frac{\partial u}{\partial n} = \frac{\partial v}{\partial n} = 0, \quad x \in \partial\Omega,\ t > 0,\\
&u(x,0) = u_0(x) \geqslant 0, \quad v(x,0) = v_0(x) \geqslant 0, \quad x \in \Omega,
\end{aligned} \tag{1}$$

where $u = u(x,t)$, $v = v(x,t)$ denote the population densities of the prey and predator at location x and time t, respectively. $d_1 > 0$ and $d_2 > 0$ are the diffusion coefficients of the prey and predator, respectively. r is the prey intrinsic growth rate. K is the carrying capacity. m is their encounter rate. c is the conversion rate of predation, and η is the death rate, respectively. r, K, m, c, η, θ_1, and θ_2 are positive. The Laplacian operator Δ describes the spatial dispersal with passive diffusion. The harvesting function

$$H(u) = \begin{cases} Eu, & 0 < u < T,\\ h, & u > T. \end{cases}$$

Here T is the harvesting threshold, $h = ET$, and E is the harvesting effort. Assume that $0 < T < 1$ to investigate the influence of the threshold harvesting. $\Omega \subset \mathbb{R}^N$ is a bounded domain with $N \geqslant 1$, and n is the normal vector that goes out of the bounded domain Ω. The homogeneous Neumann boundary conditions indicate that there is no population flux across the boundaries.

By transformations $\widetilde{u} = u/K$, $\widetilde{v} = v/K$, $\widetilde{r} = r/(mK)$, $\widetilde{\eta} = \eta/(cmK)$, $\widetilde{T} = T/K$, $\widetilde{E} = E/(mK)$, $\widetilde{h} = h/(mK^2)$, $\widetilde{\theta}_1 = K\theta_1/m$, $\widetilde{\theta}_2 = \theta_2/m$, $\widetilde{t} = mKt$, $\widetilde{x} = \sqrt{mK}x$ and dropping the tildes, (1) turns to

$$\begin{aligned}
&\frac{\partial u}{\partial t} = d_1\Delta u + ru(1-u) - uv - H(u) - \theta_1 u^3, \quad (x,t) \in \Omega \times (0,+\infty),\\
&\frac{\partial v}{\partial t} = d_2\Delta v + cv(u-\eta) - \theta_2 v^2, \quad (x,t) \in \Omega \times (0,+\infty),\\
&\frac{\partial u}{\partial n} = \frac{\partial v}{\partial n} = 0, \quad x \in \partial\Omega,\ t > 0,\\
&u(x,0) = u_0(x) \geqslant 0, \quad v(x,0) = v_0(x) \geqslant 0, \quad x \in \Omega,
\end{aligned} \tag{2}$$

and $|\Omega|$ is the Lebesgue measure of Ω.

In this paper, we aim to observe how the harvesting and toxins influence the species by exploring spatiotemporal dynamics of system (2). The full text is organised as below. In Section 2, the permanence of (2) is studied. In Section 3, the existence of nonnegative equilibria is analyzed. In Section 4, stability, Turing instability, and Turing patterns are explored. Section 5 focuses on the nonexistence, existence of special solutions, and bifurcation analysis. In Section 6, numerical simulations are shown to verify our theoretical research. Finally, we summarize our conclusions.

2 Permanence

In this section, the existence and boundedness of the solution to system (2) are proved. By utilizing the conclusion in [31] the lemma is gained below.

Lemma 1.

(i) *If $u_0(x)$ and $v_0(x)$ are nonnegative, then* (2) *has a unique solution* $(u(x,t), v(x,t))$ *such that* $u(x,t) > 0$, $v(x,t) > 0$ *with* $t \in (0,\infty)$.

(ii) *The solution* $(u(x,t), v(x,t))$ *satisfies*

$$\limsup_{t\to+\infty} \max_{x\in\overline{\Omega}} u(x,t) \leqslant 1, \qquad \limsup_{t\to+\infty} \max_{x\in\overline{\Omega}} v(x,t) \leqslant \frac{c}{\theta_2}.$$

Now, it turns out that system (2) is permanent. This means that whatever the diffusion coefficients are, both species will always exist together anytime anywhere.

Theorem 1. *If*

$$r > \max\{E, 2\sqrt{rh}\} + \frac{c}{\theta_2} + \theta_1 \quad \textit{and} \quad \eta < \max\{M_1, M_2\},$$

where

$$M_1 = \frac{(r - \frac{c}{\theta_2} - \theta_1) + \sqrt{(r - \frac{c}{\theta_2} - \theta_1)^2 - 4rh}}{2r}, \qquad M_2 = \frac{r\theta_2 - c - E\theta_2 - \theta_1\theta_2}{r\theta_2},$$

then system (2) *is permanent.*

Proof. Suppose $u_0(x) \geqslant 0$, $v_0(x) \geqslant 0$. By (2) we have

$$\frac{\partial u}{\partial t} - d_1\Delta u \geqslant ru(1-u) - u\widetilde{v} - H(u) - \theta_1\widetilde{u}^2 u, \quad x \in \Omega,\ t > 0,$$
$$\frac{\partial u}{\partial n} = 0, \quad x \in \partial\Omega,\ t > 0.$$

It implies that if $0 \leqslant u \leqslant T$ and $r - c/\theta_2 - \theta_1 > E$, then

$$\liminf_{t\to+\infty} \min_{\overline{\Omega}} u(\cdot, t) \geqslant M_2. \tag{3}$$

If $u > T$ and $r - c/\theta_2 - \theta_1 > 2\sqrt{rh}$, then

$$\liminf_{t\to+\infty} \min_{\overline{\Omega}} u(\cdot, t) \geqslant M_1. \tag{4}$$

Therefore, there exists a $t_3 > 0$, and $u(\cdot, t) > \max\{M_1, M_2\} + \varepsilon_2 := \underline{u}$ for $\varepsilon_2 > 0$, $t \in [t_3, +\infty)$.

Similarly, by (2), if $\underline{u} > \eta$, then

$$\liminf_{t\to+\infty} \overline{\Omega} \min v(\cdot, t) \geqslant \frac{c(\underline{u} - \eta)}{\theta_2}. \tag{5}$$

By Lemma 1 and (3)–(5) system (2) is permanent. □

Remark 1. Theorem 1 demonstrates that the prey and predator would exist together when the prey intrinsic rate r is larger enough, and the predator death rate η is more minor sufficiently.

3 Existence of nonnegative equilibria

Obviously, system (2) has an extinction equilibrium $E_0 = (0, 0)$. At first, we analyze the predator-free equilibrium below.

Proposition 1.

(i) *If* $0 < u_1^* \leqslant T$, $r > E$, *then system* (2) *has a unique boundary equilibrium* $E_1^* = (u_1^*, 0)$.

(ii) *If* $u_k^* > T$, $G(\hat{u}) > h$, *then system* (2) *has two boundary equilibria* $E_k^* = (u_k^*, 0)$, $k = 2, 3$; *If* $u_4^* > T$, $G(\hat{u}) = h$, *then system* (2) *has a unique boundary equilibrium* $E_4^* = (u_4^*, 0)$. *Here* $G(u) = ru(1-u) - \theta_1 u^3$, $G(\hat{u})$ *is the local maximum of* $G(u)$.

Proof. We consider roots of equation $G(u) - H(u) = 0$.

Since $H(u)$ is a piecewise function, there are equations below:

$$ru(1-u) - \theta_1 u^3 - Eu = 0 \tag{6}$$

and

$$ru(1-u) - \theta_1 u^3 - h = 0, \tag{7}$$

where $h = ET$. By (6) we get $\theta_1 u^2 + ru + (E - r) = 0$. If $0 < u_1^* \leqslant T$, $r > E$, then (6) has a unique positive solution $u_1^* = (-r + \sqrt{r^2 - 4\theta_1(E-r)})/(2\theta_1)$. If $r \leqslant E$, then (6) has no positive solution. Similarly, by the Descartes's rule, (7) has solutions u_2^*, u_3^*. It is clear that $G'(u) = r - 2ru - 3\theta_1 u^2$. Obviously, $G'(0) = r > 0$, $G'(1) = -r - 3\theta_1 < 0$, $G''(u) = -2r - 6\theta_1 u < 0$. So $G'(u) = 0$ has one positive root marked as $\hat{u} \in (0, 1)$. This indicates that $G(u)$ has different monotonicity in $(0, \hat{u})$ and $(\hat{u}, 1)$. Its local maximum is $G(\hat{u})$ in $(0, 1)$. Thus, (7) has two positive roots as $G(\hat{u}) > h$, a positive root as $G(\hat{u}) = h$, and no positive roots as $G(\hat{u}) < h$. The number of positive roots in $(0, 1)$ for different θ_1 and h are shown in Fig. 1(a). All possible equilibria are denoted as $E_k^* = (u_k^*, 0)$, $k = 1, 2, 3, 4$. □

Remark 2. From the above results, if $r > E$ or $h \leqslant G(\hat{u})$, then system (2) always exists the boundary equilibrium. So the threshold harvesting and the toxins increase the system complexity. We can find that under the threshold harvesting and the toxins, system (2) possesses from zero to four boundary equilibria, but it has at most two boundary equilibria without threshold harvesting.

Next, we analyze the interior equilibrium.

Proposition 2.

(i) *If* $0 < u^* \leqslant T$ *and* $r + c\eta/\theta_2 > E$, *then system* (2) *has a unique interior equilibrium* $E^* = (u^*, v^*)$.

(ii) *If* $u_k^* > T$ *and* $R(\tilde{u}) > h$, *then system* (2) *has two interior equilibria* $E_k^* = (u_k^*, v_k^*)$, $k = 2, 3$; *If* $u_4^* > T$ *and* $R(\tilde{u}) = h$, *then system* (2) *has a unique interior equilibrium* $E_4^* = (u_4^*, v_4^*)$. *Here* $R(u) = (r + c\eta/\theta_2)u - (r + c/\theta_2/u^2 - \theta_1 u^3$, $R(\tilde{u})$ *is the local maximum of* $R(u)$.

The proof is omitted, it is analogous to that of Proposition 1. The number of positive roots in $(0, 1)$ for different h is shown in Fig. 1(b).

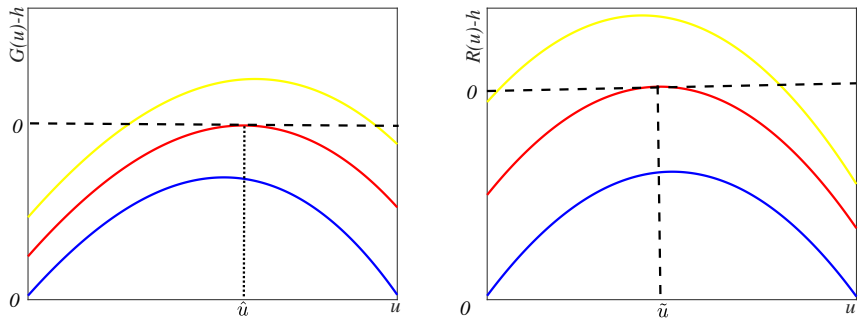

(a) (b)

Figure 1. The number of positive roots in $(0, 1)$ for different θ_1 and h.

Remark 3. With the above derivation, if the harvesting effect E is smaller enough than the prey intrinsic growth rate r, then the prey and the predator can coexist.

4 Stability and Turing patterns

4.1 Local stability

In this section, the local stability of system (2) is discussed. System (2) can be rewritten as

$$\begin{aligned} \frac{\partial u}{\partial t} &= d_1\Delta u + ru(1-u) - uv - \theta_1 u^3 - \big[Eu + \rho(h - Eu)\big], \\ \frac{\partial v}{\partial t} &= d_2\Delta v + cv(u-\eta) - \theta_2 v^2, \end{aligned} \tag{8}$$

where

$$\rho = \begin{cases} 0, & 0 \leqslant u \leqslant T, \\ 1, & u > T. \end{cases}$$

By linearization (8) reduces to

$$\begin{pmatrix} \phi_t \\ \psi_t \end{pmatrix} = L \begin{pmatrix} \phi \\ \psi \end{pmatrix} = D \begin{pmatrix} \Delta\phi \\ \Delta\psi \end{pmatrix} + J(u^*, v^*) \begin{pmatrix} \phi \\ \psi \end{pmatrix},$$

where

$$D = \begin{pmatrix} d_1 & 0 \\ 0 & d_2 \end{pmatrix}, \qquad J(u^*, v^*) = \begin{pmatrix} A(u^*, v^*) & B(u^*, v^*) \\ C(u^*, v^*) & D(u^*, v^*) \end{pmatrix}.$$

$$\begin{aligned} &A(u^*, v^*) = r - 2ru^* - v^* - 3\theta_1 {u^*}^2 - (1-\rho)E, \\ &B(u^*, v^*) = -u^*, \qquad C(u^*, v^*) = cv^*, \\ &D(u^*, v^*) = cu^* - c\eta - 2\theta_2 v^*. \end{aligned}$$

Let $0 = \mu_0 < \mu_1 < \mu_2 < \cdots < \mu_k < \cdots \to \infty$ be the eigenvalues of $-\Delta$ on Ω. Define

(i) $S(\mu_i)$ is the space of eigenfunctions with $\mu_i \in C^1(\overline{\Omega})$ for $i = 1, 2, 3, \ldots, m(\mu_i)$ is the algebraic multiplicity of μ_i, that is, $m(\mu_i) = \dim S(\mu_i)$;

(ii) $X_{ij} := \{\mathbf{c}\phi_{ij}\colon\ \mathbf{c} \in \mathbb{R}^2\}$, where $\{\phi_{ij}\}$ is the orthonormal base of $S(\mu_i)$ for $j = 1, 2, 3, \ldots$, $\mathbf{c}$ is the constant vector;

(iii) $X := \{(u, v) \in [C^1(\overline{\Omega})]^2\colon\ \partial u/\partial n = \partial v/\partial n = 0\}$, $X_i = \oplus_{j=1}^{m(\mu_i)} X_{ij}$, and $X = \oplus_{i=1}^{\infty} X_i$, X_i is the invariant set of operator L.

If λ is an eigenvalue of operator L, then it must be an eigenvalue of matrix $-\mu_i D + J(u^*, v^*)$ for each $i \geqslant 0$. Thus, we consider characteristic equation

$$\lambda^2 - T_i\lambda + D_i = 0, \quad i \in N_0, \tag{9}$$

where

$$\begin{aligned} T_i &= -\mu_i(d_1+d_2)+A(u^*,v^*)+D(u^*,v^*),\\ D_i &= d_1d_2\mu_i^2-\big[A(u^*,v^*)d_2+D(u^*,v^*)d_1\big]\mu_i\\ &\quad+\big[A(u^*,v^*)D(u^*,v^*)-B(u^*,v^*)C(u^*,v^*)\big]\\ &=\big[d_1\mu_i-A(u^*,v^*)\big]\big[d_2\mu_i-D(u^*,v^*)\big]-B(u^*,v^*)C(u^*,v^*). \end{aligned}$$

Obviously, if $r<E$, then

$$A(0,0)=r-E,\qquad B(0,0)=C(0,0)=0,\qquad D(0,0)=-c\eta.$$

So the steady state $(0,0)$ is stable.

If $0<u_1^*\leqslant T$, $r>E$, where $u_1^*=(-r+\sqrt{r^2+4\theta_1(r-E)})/(2\theta_1)$,

$$A(u_1^*,0)=r-2ru_1^*-3\theta_1\,u_1^{*2}-E<0,\qquad B(u_1^*,0)=-u_1^*,$$
$$C(u_1^*,0)=0,\qquad D(u_1^*,0)=cu_1^*-c\eta,$$

and $u_1^*<\eta$, then $T_i<0$, $D_i>0$, and the steady state $(u_1^*,0)$ is stable.

By similar analysis, if $u_i^*>T$ $(i=2,3)$, $G(\hat{u})>h$, and $T_i<0$, $D_i>0$, then the steady states $(u_i^*,0)$ $(i=2,3)$ are stable. If $T_i<0$, $D_i>0$, then the steady state $(u_4^*,0)$ is stable.

Next, the stability of the positive equilibrium can be gained. If $0<u^*\leqslant T$, $r+cm\eta/\theta_2>E$, then (2) has one unique positive solution (u^*,v^*). Since

$$A(u^*,v^*)<0,\qquad B(u^*,v^*)=-u^*,\qquad C(u^*,v^*)=cv^*,\qquad D(u^*,v^*)<0,$$

so the steady state (u^*,v^*) is stable.

If $\bar{u}_i^*>T$ $(i=2,3)$, $R(\tilde{u})>h$, and

$$A(\bar{u}_i^*,\bar{v}_i^*)<0,\qquad B(\bar{u}_i^*,\bar{v}_i^*)=-\bar{u}_i^*,\qquad C(\bar{u}_i^*,\bar{v}_i^*)=c\bar{v}_i^*,\qquad D(\bar{u}_i^*,\bar{v}_i^*)<0,$$

then $(\bar{u}_i^*,\bar{v}_i^*)$ $(i=2,3)$ are stable.

If $\bar{u}_4^*>T$, $R(\tilde{u})=h$, and

$$A(\bar{u}_4^*,\bar{v}_4^*)<0,\qquad D(\bar{u}_4^*,\bar{v}_4^*)<0,$$

then the steady state $(\bar{u}_4^*,\bar{v}_4^*)$ is also stable.

So the results below can be obtained according to the above discussion.

Theorem 2. *The following statements are true for system* (2):

(i) *If $r<E$, then the extinct equilibrium point $(0,0)$ is stable.*

(ii) *If $0<u_1^*<\max\{T,\eta\}$, $r>E$, and $A(u_1^*,0)<0$, then the boundary equilibrium point $(u_1^*,0)$ is stable*; *If $T<u_i^*<\eta$ $(i=2,3)$, $G(\hat{u})>h$, and $A(u_i^*,0)<0$, then $(u_i^*,0)$ $(i=2,3)$ are stable*; *If $T<u_4^*<\eta$, $G(\hat{u})=h$, and $A(u_4^*,0)<0$, then $(u_4^*,0)$ is stable.*

(iii) *If* $0 < u^* \leqslant T$, $r + cm\eta/\theta_2 > E$, $A(u^*, v^*) < 0$, *and* $D(u^*, v^*) < 0$, *then* (u^*, v^*) *is stable*; *If* $\bar{u}_i^* > T$ $(i = 2, 3)$, $R(\tilde{u}) > h$, $A(\bar{u}_i^*, \bar{v}_i^*) < 0$, *and* $D(\bar{u}_i^*, \bar{v}_i^*) < 0$, *then* $(\bar{u}_i^*, \bar{v}_i^*)$ $(i = 2, 3)$ *are stable*; *If* $\bar{u}_4^* > T$, $R(\tilde{u}) = h$, $A(\bar{u}_4^*, \bar{v}_4^*) < 0$, $D(\bar{u}_4^*, \bar{v}_4^*) < 0$, *then the steady state* $(\bar{u}_4^*, \bar{v}_4^*)$ *is also stable.*

Remark 4. From the above content, when the harvesting effort E is bigger than the prey intrinsic growth rate r, two species can be extinct. When the harvesting effort E is smaller than the prey intrinsic growth rate r and the threshold T is larger enough, the prey can exist, but the predator can be extinct. When the harvesting effort E is smaller sufficient than the prey intrinsic growth rate r, two species can coexist.

4.2 Global stability

In the following, we obtain the global asymptotic stability of the trivial steady state solution by constructing a suitable Lyapunov functional.

Theorem 3. *If*

$$r < E, \quad r - 2rT - 3\theta_1 T^2 < 0, \quad \textit{and} \quad rT(1-T) - \theta_1 T^3 < h,$$

then the trivial steady state $(0, 0)$ *is globally asymptotically stable for system* (2).

Proof. Define the following Lyapunov functional:

$$W(u, v) = \int_\Omega u \,\mathrm{d}x + \frac{1}{c} \int_\Omega v \,\mathrm{d}x.$$

Then

$$\begin{aligned}
&\frac{\mathrm{d}}{\mathrm{d}t} W\big(u(x,t), v(x,t)\big) \\
&\quad = \int_\Omega \left[ru(1-u) - uv - H(u) - \theta_1 u^3\right] \mathrm{d}x + \frac{1}{c} \int_\Omega \left(cuv - c\eta v - \theta_2 v^2\right) \mathrm{d}x \\
&\quad = \int_\Omega \left[ru(1-u) - H(u) - \theta_1 u^3\right] \mathrm{d}x - \frac{1}{c} \int_\Omega \left(c\eta v + \theta_2 v^2\right) \mathrm{d}x.
\end{aligned}$$

It can be obtained from those conditions $r < E$, $r - 2rT - 3\theta_1 T^2 < 0$, $rT(1-T) - \theta_1 T^3 < h$ for all $u \geqslant 0$,

$$ru(1-u) - \theta_1 u^3 \leqslant H(u).$$

Thus, $\mathrm{d}W(u, v)/\mathrm{d}t$ is nonnegative and the derivative is zero if and only if $(u, v) = (0, 0)$. So the trivial steady state $(0, 0)$ to (2) is globally asymptotically stable by [5] and Theorem 2. □

Remark 5. Theorem 3 means that two species will be extinct as E and T are larger enough. So the lower harvesting can lead to population survival.

4.3 Turing instability

In the subsection, the necessary conditions for the emergence of Turing instability are given. It is well known that once the prey density diffuses more slowly, so Turing instability occurs.

At first, we consider the following system:

$$\begin{aligned} \frac{\mathrm{d}u}{\mathrm{d}t} &= ru(1-u) - uv - H(u) - \theta_1 u^3, \\ \frac{\mathrm{d}v}{\mathrm{d}t} &= cv(u-\eta) - \theta_2 v^2. \end{aligned} \tag{10}$$

It is known that if a positive steady state solution $E^* = (u^*, v^*)$ is an asymptotically stable state to system (10), but is unstable with respect to the solution to spatial system (2), then Turing instability occurs. Denoting

$$k_1 = \frac{\Delta_1 - \sqrt{\Delta_1^2 + \Delta_2}}{2d_1 d_2}, \qquad k_2 = \frac{\Delta_1 + \sqrt{\Delta_1^2 + \Delta_2}}{2d_1 d_2},$$

where

$$\begin{aligned} \Delta_1 &= \big[A(u^*, v^*)d_2 + D(u^*, v^*)d_1\big], \\ \Delta_2 &= 4d_1 d_2\big[A(u^*, v^*)D(u^*, v^*) - B(u^*, v^*)C(u^*, v^*)\big], \end{aligned}$$

and we can obtain the following results.

Theorem 4. *Assume that the following conditions hold*:

$$A(u^*, v^*) + D(u^*, v^*) < 0, \tag{11}$$

$$A(u^*, v^*)D(u^*, v^*) - B(u^*, v^*)C(u^*, v^*) > 0, \tag{12}$$

$$A(u^*, v^*)d_2 + D(u^*, v^*)d_1 < 0, \tag{13}$$

$$0 < \frac{d_1}{d_2} < \frac{\Delta_3 - \sqrt{\Delta_3^2 - A^2(u^*, v^*)D^2(u^*, v^*)}}{D^2(u^*, v^*)}. \tag{14}$$

Then the positive constant steady state solution $E^* = (u^*, v^*)$ *of system* (2) *is Turing unstable if* $0 < k_1 < \mu_i < k_2$ *for some* μ_i*, where*

$$\Delta_3 = A(u^*, v^*)D(u^*, v^*) - 2B(u^*, v^*)C(u^*, v^*).$$

Proof. According to the previous discussions, the characteristic equation of system (10) at the positive steady state solution $E^* = (u^*, v^*)$ is as follows:

$$\begin{aligned} \lambda^2 &- \big[A(u^*, v^*) + D(u^*, v^*)\big]\lambda \\ &+ \big[A(u^*, v^*)D(u^*, v^*) - B(u^*, v^*)C(u^*, v^*)\big] = 0, \end{aligned}$$

the positive steady state solution $E^* = (u^*, v^*)$ of system (10) is asymptotically stable if conditions (11)–(14) hold.

For spatial system (2), we have

$$\begin{aligned} D_i &= \big[d_1\mu_i - A(u^*,v^*)\big]\big[d_2\mu_i - D(u^*,v^*)\big] - B(u^*,v^*)C(u^*,v^*) \\ &= d_1d_2{\mu_i}^2 - \big[d_1D(u^*,v^*) + d_2A(u^*,v^*)\big]\mu_i \\ &\quad + A(u^*,v^*)D(u^*,v^*) - B(u^*,v^*)C(u^*,v^*). \end{aligned}$$

If there exists a μ_i such that $0 < k_1 < \mu_i < k_2$, then $D_i < 0$. Therefore, D_i takes the minimum value at $\mu_i = \mu_{\min} = (d_1D(u^*,v^*) + d_2A(u^*,v^*))/(2d_1d_2)$ when $d_1D(u^*,v^*) + d_2A(u^*,v^*) > 0$. This condition implies that

$$\frac{D^2(u^*,v^*)}{A^2(u^*,v^*)}\frac{d_1^2}{d_2^2} + \frac{4B(u^*,v^*)C(u^*,v^*) - 2A(u^*,v^*)D(u^*,v^*)}{A^2(u^*,v^*)}\frac{d_1}{d_2} + 1 > 0. \tag{15}$$

Hence, D_i is negative. Thus, (15) is the criteria for Turing instability of system (2). From (15) we have

$$0 < \frac{d_1}{d_2} < \frac{\Delta_3 - \sqrt{\Delta_3^2 - A^2(u^*,v^*)D^2(u^*,v^*)}}{D^2(u^*,v^*)},$$

denoting $\Delta_3 = A(u^*,v^*)D(u^*,v^*) - 2B(u^*,v^*)C(u^*,v^*)$, which means that one eigenvalue of Eq. (9) has positive real part, thus Turing instability occurs. □

4.4 Turing patterns

Here we analyze the patterns and judge their stability. Now assume that $E^* = (u^*, v^*)$ is an internal equilibrium. Let

$$u = u^* + \varepsilon_1, \qquad v = v^* + \varepsilon_2. \tag{16}$$

Substituting (16) into system (2) and by the Taylor expansion, the linear perturbation equations are obtained as follows:

$$\frac{\partial A}{\partial t} = JA + DLA, \tag{17}$$

where

$$A = \begin{pmatrix} \varepsilon_1 \\ \varepsilon_2 \end{pmatrix}, \qquad J = \begin{pmatrix} A(u^*,v^*) & B(u^*,v^*) \\ C(u^*,v^*) & D(u^*,v^*) \end{pmatrix},$$
$$D = \begin{pmatrix} d_1 & 0 \\ 0 & d_2 \end{pmatrix}, \qquad L = \begin{pmatrix} \Delta & 0 \\ 0 & \Delta \end{pmatrix}.$$

Let

$$\begin{pmatrix} \varepsilon_1 \\ \varepsilon_2 \end{pmatrix} = \sum_{q=1}^{3} \begin{pmatrix} c_q^1 \\ c_q^2 \end{pmatrix} \exp(\lambda_k t + \mathrm{i}\mathbf{k}\cdot\mathbf{r}), \tag{18}$$

where λ_k is the growth rate of perturbations, i is the imaginary unit, $\mathbf{k}$ is the wave number, and $\mathbf{r}$ is the directional vector.

Substitute Eq. (18) into the perturbation equation (17) to obtain the characteristic equation

$$\lambda_k \begin{pmatrix} c_q^1 \\ c_q^2 \end{pmatrix} = \begin{pmatrix} A(u^*, v^*) - k^2 d_1 & B(u^*, v^*) \\ C(u^*, v^*) & D(u^*, v^*) - k^2 d_2 \end{pmatrix} \begin{pmatrix} c_q^1 \\ c_q^2 \end{pmatrix}.$$

So dispersion relation is

$$\lambda_k^2 - \mathrm{tr}_k\, \lambda_k + \Delta_k = 0, \tag{19}$$

the solutions of Eq. (19) are $\lambda_k = (\mathrm{tr}_k \pm \sqrt{\mathrm{tr}_k^2 - 4\Delta_k})/2$, which determine the stability of Eq. (17), and where

$$\begin{aligned} \mathrm{tr}_k &= A(u^*, v^*) + D(u^*, v^*) - k^2(d_1 + d_2) \\ &= \mathrm{tr}(J) - k^2(d_1 + d_2), \\ \Delta_k &= A(u^*, v^*)D(u^*, v^*) - B(u^*, v^*)C(u^*, v^*) \\ &\quad - k^2\big[D(u^*, v^*)d_1 + A(u^*, v^*)d_2\big] + k^4 d_1 d_2. \end{aligned}$$

Conditions for the occurrence of Hopf bifurcation are $\mathrm{Re}(\lambda_k) = 0$ and $\mathrm{Im}(\lambda_k) \neq 0$. So $\mathrm{tr}(J) \equiv 0$, $\det(J) > 0$, $k = 0$, and $\partial\,\mathrm{Re}(\lambda)/\partial d_1 \neq 0$. While $\lambda_0 = (\mathrm{tr}_0 \pm \sqrt{\mathrm{tr}_0^2 - 4\Delta_0})/2 < 0$ and $\Delta_k < 0$ are conditions for the occurrence of Turing bifurcation, which requires

$$\mathrm{tr}_0 < 0, \qquad \Delta_0 > 0.$$

Minimize $\Delta_k = 0$ for $k = k_T > 0$ with

$$k_T^2 = \frac{D(u^*, v^*)d_1 + A(u^*, v^*)d_2}{2d_1 d_2}. \tag{20}$$

Afterwards, substitute Eq. (20) into $\Delta_k = 0$ and get

$$\Delta_{k_T} = \Delta_0 - \frac{\big[D(u^*, v^*)d_1 + A(u^*, v^*)d_2\big]^2}{4d_1 d_2} = 0,$$

which is

$$k_T^2 = \sqrt{\frac{\Delta_0}{d_1 d_2}} = \sqrt{\frac{A(u^*, v^*)D(u^*, v^*) - B(u^*, v^*)C(u^*, v^*)}{d_1 d_2}}. \tag{21}$$

So we get the critical value of Turing bifurcation parameter

$$d_{1T} = \frac{\Delta + \sqrt{\Delta^2 - 4A^2(u^*, v^*)D^2(u^*, v^*)d_2^2}}{2D^2(u^*, v^*)}$$

about d_1 by substituting Eq. (21) into $\Delta_k = 0$, where

$$\Delta = [A(u^*, v^*)D(u^*, v^*) - B(u^*, v^*)C(u^*, v^*)]d_2.$$

Now we judge the stability of different patterns by dividing the control parameter interval for these patterns. For these purposes, we analyze the amplitude equation. To get it, we need the multiple scale method in [20]. Select d_1 as a control parameter and d_{1T} as the bifurcation threshold. Patterns of (2) can be described as the models of wave vectors $(\mathbf{k_j}, -\mathbf{k_j})$ $(j = 1, 2, 3)$ intersecting with each other of $2\pi/3$ and $|\mathbf{k_j}| = k_T$.

Each stable steady Turing pattern corresponds to a solution, and each amplitude A_i can be written as $A^i = \rho_i \exp(\mathrm{i}\theta_i)$ in which $\rho_i = |A^i|$ and φ_i are the phase angles of A_i. Subsequently, substitute $A^i = \rho_i \exp(\mathrm{i}\theta_i)$ into system

$$\tau_0 \frac{\partial \varphi}{\partial t} = -h \frac{\rho_1^2\rho_2^2 + \rho_1^2\rho_3^2 + \rho_2^2\rho_3^2}{\rho_1\rho_2\rho_3}, \tag{22}$$

$$\tau_0 \frac{\partial \rho_1}{\partial t} = \mu\rho_1 + h\rho_2\rho_3 \cos\theta - \big(g_1\rho_1^2 + g_2\big(\rho_2^2 + \rho_3^2\big)\big)\rho_1^2, \tag{23}$$

$$\tau_0 \frac{\partial \rho_2}{\partial t} = \mu\rho_2 + h\rho_1\rho_3 \cos\theta - \big(g_1\rho_2^2 + g_2\big(\rho_1^2 + \rho_3^2\big)\big)\rho_2^2, \tag{24}$$

$$\tau_0 \frac{\partial \rho_3}{\partial t} = \mu\rho_3 + h\rho_1\rho_2 \cos\theta - \big(g_1\rho_3^2 + g_2\big(\rho_2^2 + \rho_3^2\big)\big)\rho_1^2 \tag{25}$$

in which $\theta = \theta_1 + \theta_2 + \theta_3$. The system composed of Eqs. (22)–(25) has five solutions.

The first solution is $\rho_1 = \rho_2 = \rho_3 = 0$, which always exists and will be unstable when μ satisfies $\mu < \mu_2 = 0$. The second solution to the system is $\rho_1 = \sqrt{\mu/g_1}$, $\rho_2 = \rho_3 = 0$, which exists when $\mu > \mu_2 = 0$ is satisfied and will be stable when $\mu > \mu_3 = h^2 g_1/(g_1 - g_2)^2$ corresponding to stripe patterns. When $\mu > \mu_1$ is held, we have the other two solutions: $\rho_1 = \rho_2 = \rho_3 = (|h| \pm \sqrt{h^2 + 4(g_1 + 2g_2)\mu})/(2(g_1 + 2g_2))$, which are spot patterns. We mark $(|h| + \sqrt{h^2 + 4(g_1 + 2g_2)\mu})/(2(g_1 + 2g_2))$ and $(|h| - \sqrt{h^2 + 4(g_1 + 2g_2)\mu})/(2(g_1 + 2g_2))$ by ρ_i^+ and ρ_i^-, respectively. The former solution ρ_i^+ is stable as $\mu < \mu_4$, while ρ_i^- is unstable. The mixed patterns are $\rho_1 = |h|/(g_2 - g_1)$, $\rho_2 = \rho_3 = \sqrt{(\mu - g_1\rho_1^2)/(g_1 + g_2)}$, which exist when $g_2 > g_1$ is satisfied, but are always unstable. See the detailed derivation process in [29].

5 Steady state solutions

Now the conditions for some special solutions will be discussed. The elliptic system is

$$\begin{aligned} &-d_1\Delta u = ru(1-u) - uv - H(u) - \theta_1 u^3, \quad x \in \Omega, \\ &-d_2\Delta v = cv(u - \eta) - \theta_2 v^2, \quad x \in \Omega, \\ &\frac{\partial u}{\partial n} = \frac{\partial v}{\partial n} = 0, \quad x \in \partial\Omega. \end{aligned} \tag{26}$$

The solutions below refer to the classical solutions in $C^2(\Omega)\bigcap C^1(\overline{\Omega})$. From [30] Theorems 5 and 6 are gained, where the detailed derivation processes are analogous to [30]. So we omit them.

5.1 Predator-free nonconstant solutions

In this subsection, the predator-free nonconstant solutions to system (26) are considered:

$$\begin{aligned} &-d_1\Delta u = ru(1-u) - H(u) - \theta_1 u^3, \quad x \in \Omega, \\ &\frac{\partial u}{\partial n} = 0, \quad x \in \partial\Omega. \end{aligned} \tag{27}$$

First, the following maximum principle [15] is introduced.

Lemma 2. *Let the bounded Lipschitz domain $\Omega \in \mathbb{R}^n$ and $g \in C(\overline{\Omega} \times \mathbb{R})$. Suppose $Z \in H^1(\Omega)$ is a weak solution to the inequalities*

$$\begin{aligned} &\Delta z + g\big(x, z(x)\big) \geqslant 0, \quad x \in \Omega, \\ &\frac{\partial z}{\partial n} \leqslant 0, \quad x \in \partial\Omega, \end{aligned}$$

and there exists a constant K such that $g(x,z) < 0$ for $z > K$, then $z \leqslant K$ a.e. in Ω.

Theorem 5. *If μ_i, $i \in N_0$, are the eigenvalues of $-\Delta$, then the following statements are factual*:

(i) *All nontrivial solutions to system* (27) *satisfy* $0 < u < 1$.
(ii) *If* $\widetilde{d_1} = r + E + 3\theta_1 K^2$ *with* $d_1 > \widetilde{d_1}$, *then system* (27) *has no nonconstant steady state solutions.*

5.2 Nonexistence of nonconstant positive solutions

In this subsection, the nonexistence of nonconstant positive solutions to system (26) will be analyzed.

Lemma 3. *If $(u(x), v(x))$ is a nonnegative solution to system* (26), *then $(u(x), v(x))$ is a predator-free solution to* (27), *or it meets $0 < u(x) < 1$, $0 < v(x) < c/\theta_2$.*

Theorem 6. *If*

$$d^* = \max\left\{\frac{A_1}{\mu_1}, \frac{A_2}{\mu_2}\right\} \quad \textit{and} \quad d^* < \min\{d_1, d_2\},$$

where

$$A_1 = r + E + 3\theta_1 K^2 + \frac{m}{2} + \frac{c^2}{2\theta_2}, \qquad A_2 = \frac{m}{2} + c + \frac{c^2}{2\theta_2} - c\eta,$$

then system (26) *has no nonconstant solutions.*

5.3 Existence of nonconstant positive solutions

While other parameters are fixed as the diffusion coefficients d_1 and d_2 are changed, we study the existence of these solutions to system (26) by the Leray–Schauder degree theory.

Denote $\mathbf{u} = (u, v)$ and

$$\Phi(\mathbf{u}) = \begin{pmatrix} ru(1-u) - uv - H(u) - \theta_1 u^3 \\ cv(u-\eta) - \theta_2 v^2 \end{pmatrix},$$

then (26) can be rewritten as

$$\begin{aligned} &-D\Delta\mathbf{u} = \Phi(\mathbf{u}), \quad x \in \Omega, \\ &\frac{\partial \mathbf{u}}{\partial n} = 0, \quad x \in \partial\Omega, \end{aligned}$$

or equivalently,

$$\mathbf{F}(\mathrm{d}_1, \mathrm{d}_2; \mathbf{u}) = \mathbf{u} - (I - \Delta)^{-1}\big\{D^{-1}\Phi(\mathbf{u}) + \mathbf{u}\big\} = 0, \tag{28}$$

where $(I - \Delta)^{-1}$ is the inverse of $I - \Delta$ with the homogeneous Neumann boundary conditions.

From (28) we have

$$\mathbf{F}_{\mathbf{u}}(E^*) = I - (I - \Delta)^{-1}\big\{D^{-1}\mathbf{F}_{\mathbf{u}}(E^*) + I\big\} = 0,$$

where E^* is the unique positive constant steady state solution to (2). So

$$\operatorname{index}\big(F(\cdot), E^*\big) = (-1)^{\gamma},$$

where γ is the number of negative eigenvalues of $\mathbf{F}_{\mathbf{u}}(E^*)$. λ is an eigenvalue of the matrix

$$B_j = I - \frac{1}{1+\mu_j}\big[D^{-1}\Phi_{\mathbf{u}}(E^*) + I\big] = \frac{1}{1+\mu_j}\big[\mu_j I - D^{-1}\Phi_{\mathbf{u}}(E^*)\big].$$

Denote

$$H(d_1, d_2; \mu) = \det\big[\mu I - D^{-1}\Phi_{\mathbf{u}}(E^*)\big] = \frac{1}{d_1 d_2}\det\big[\mu D - \Phi_{\mathbf{u}}(E^*)\big], \tag{29}$$

which means that if $H(d_1, d_2; \mu) \neq 0$, then $H(d_1, d_2; \mu)$ is negative as the number of negative eigenvalues of $\mathbf{F}_{\mathbf{u}}(E^*)$ is odd.

Lemma 4. *Suppose $H(d_1, d_2; \mu) \neq 0$ for all $i \geqslant 0$, then*

$$\operatorname{index}\big(F(\cdot), E^*\big) = (-1)^{\gamma}, \qquad \gamma = \sum_{i \geqslant 0,\ H(d_1, d_2; \mu) < 0} m(\mu_i),$$

where $m(\mu_i)$ is the algebraic multiplicity of μ_i.

By the direct calculation we have

$$\begin{aligned} \det\big[\mu D - \Phi_{\mathbf{u}}(E^*)\big] &= d_1 d_2 \mu^2 - \big(A(u^*, v^*)d_2 + D(u^*, v^*)d_1\big)\mu \\ &\quad + A(u^*, v^*)D(u^*, v^*) - B(u^*, v^*)C(u^*, v^*) \\ &= 0. \end{aligned} \tag{30}$$

Obviously, nonnegative roots of (29) exist as

$$\begin{aligned}&\big(A(u^*,v^*)d_2+D(u^*,v^*)d_1\big)^2\\&\quad-4\big(A(u^*,v^*)D(u^*,v^*)-B(u^*,v^*)C(u^*,v^*)\big)>0\\&A(u^*,v^*)d_2+D(u^*,v^*)d_1>0.\end{aligned}$$

Assume that μ^+,μ^- are two roots of (29), and the following conclusion is established.

Theorem 7. *Assume that $A(u^*,v^*)d_2+D(u^*,v^*)d_1>0$ and there exist $i,j\in N$ such that $0\leqslant\mu_j<\mu^-<\mu_{j+1}\leqslant\mu_i<\mu^+<\mu_{i+1}$, and $\sum_{k=j+1}^{i}m(\mu_k)$ is odd, then* (26) *has at least one nonconstant positive solution.*

Proof. Define

$$A_t(\mathbf{u})\triangleq(-\Delta+I)^{-1}\begin{pmatrix}u+(\frac{1-t}{d^*}+\frac{t}{d_1})f_1(u,v)\\v+(\frac{1-t}{d^*}+\frac{t}{d_1})f_2(u,v)\end{pmatrix},$$

where d^* is defined in Theorem 6, and $t\in[0,1]$.

The positive solutions to the problem

$$A_t(\mathbf{u})=\mathbf{u}\ \text{in}\ \Omega,\qquad\frac{\partial u}{\partial n}=0\ \text{on}\ \partial\Omega$$

are contained in $\Lambda=\{(u,v)\in X\colon C^{-1}<u,v<C\,\text{on}\,\Omega\}$. Note that $\mathbf{u}$ is a positive solution to system (26) if and only if it is a positive solution of (30) with $t=1$. $\mathbf{u}^*$ is the unique positive constant solution to (30) for any $t\in[0,1]$. According to the choice of d^* in Theorem 6, we have that E^* is the only fixed point of A_0.

$$\deg(I-A_0,\,\Lambda,\,0)=\deg(I-A_0,\,E^*)=1$$

since $F=I-H(\cdot,1)$. If (26) has no other solutions, except the constant one E^*, then we have

$$\deg\big(I-A_1,\,\Lambda,\,(0,0)\big)=\deg(F,E^*)=(-1)^{\sum_{k=j+1}^{i}m(\mu_k)}=-1.$$

On the other hand, by the homotopy invariance of the topological degree

$$\deg(I-A_0,\,\Lambda,\,0)=\deg(I-A_1,\,\Lambda,\,0).$$

The result is contradicted and therefore the theorem holds. □

Remark 6. Theorem 7 implies that diffusion terms can cause steady states to system (26) under certain parametric restrictions as d_2 is larger enough.

5.4 Bifurcation

In this section, the bifurcation of (2) and (26) is investigated. Let other parameters be fixed and consider $d_2>0$ as the bifurcation parameter.

From (9), if there exist an integer $k_0\geqslant0$ and $d_2^*>0$ such that

$$T_{k_0}(d_2^*)=0,\quad D_{k_0}(d_2^*)>0,\quad T_k(d_2^*)\neq0,\quad D_k(d_2^*)\neq0,\quad k\neq k_0,$$

and for the unique pair of complex eigenvalue $\alpha(d_2) \pm \mathrm{i}\omega(d_2)$ of (9), the derivative $\alpha'(d_2^*) \neq 0$, then (d_2^*, E^*) is Hopf bifurcation point. This implies that a lot of spatially periodic solutions emanate from E^*.

If there exist k_0 and $d_2^s > 0$ such that

$$D_{k_0}\big(d_2^s\big) = 0, \quad T_k\big(d_2^s\big) \neq 0, \quad D_k\big(d_2^s\big) \neq 0, \quad k \neq k_0,$$

and the derivative $D'_{k_0}(d_2^s) \neq 0$, then (d_2^s, E^*) is a point of steady state bifurcation.

Theorem 8. *Assume that $B(u^*, v^*)C(u^*, v^*) < A(u^*, v^*)D(u^*, v^*)$, then conclusions below are factual.*

(i) *If $A(u^*, v^*)+D(u^*, v^*) > 0$ and $\mu_k(d_1+d_2)-A(u^*, v^*)-D(u^*, v^*) > 0$, then E^* is unstable for any $d_2 > 0$. If there exist β_1^*, β_2^*, and $A(u^*, v^*)+D(u^*, v^*) = 0$ when $\beta_1 = \beta_1^*$, $\beta_2 = \beta_2^*$, then the Hopf bifurcation occurs at E^*, and there are homogeneous periodic solutions near E^*.*

(ii) *Let k_0 be the largest positive integer as $\mu_k(d_1+d_2)-A(u^*, v^*)-D(u^*, v^*) > 0$, and $d_{k_1} \neq d_{k_2} (k_1 \neq k_2)$, $1 \leqslant k_1, k_2 < k_0$. If $0 < A(u^*, v^*) + D(u^*, v^*) < d_1\mu_1$, then (d_{2k}^S, E^*) is the steady state bifurcation point, where*

$$d_{2k}^S = \frac{B(u^*, v^*)C(u^*, v^*)}{[d_1\mu_k - A(u^*, v^*)]\mu_k} + \frac{D(u^*, v^*)}{\mu_k}, \quad 1 \leqslant k \leqslant k_0. \tag{31}$$

(iii) *Let k_0 be defined as in (ii), $\overline{d}_2 = \min_{1\leqslant k\leqslant k_0} d_k$, $d_{2k_1} \neq d_{2k_2}$ whenever $k_1 \neq k_2$, $1 \leqslant k_1, k_2 \leqslant k_0$, then (d_{2k}^S, E^*) is the steady state bifurcation point, and E^* is unstable with $0 < d_2 < \overline{d}_2$.*

(iv) *Let k_0 be defined as in (ii), and $d_{2k_1} \neq d_{2k_2}$ whenever $k_1 \neq k_2$, $1 \leqslant k_1, k_2 \leqslant k_0$. If $0 < A(u^*, v^*) + D(u^*, v^*) < d_1\mu_1$, $B(u^*, v^*)C(u^*, v^*) < 0$, then (d_{2k}^S, E^*) is the steady state bifurcation point. If*

$$\max\left\{\frac{A(u^*, v^*) - \sqrt{-B(u^*, v^*)C(u^*, v^*)}}{d_1}, \frac{A(u^*, v^*) + D(u^*, v^*)}{2d_1}\right\}$$
$$< \mu_1 < \min\left\{\frac{A(u^*, v^*) + \sqrt{-B(u^*, v^*)C(u^*, v^*)}}{d_1}, \frac{A(u^*, v^*)}{d_1}\right\},$$

then (d_{2k}^H, E^*) is Hopf bifurcation point for $1 \leqslant k \leqslant k_0$, where

$$d_{2k}^H = \frac{A(u^*, v^*) + D(u^*, v^*)}{\mu_k} - d_1.$$

Proof. (i) From the assumption and by (9), for any $d_2 > 0$, $k \geqslant 1$, we have

$$-T_k(d_2) = \mu_k(d_1 + d_2) - A(u^*, v^*) - D(u^*, v^*) > 0,$$
$$D_k(d_2) = \big(d_1\mu_k - A(u^*, v^*)\big)\big(d_2\mu_k - D(u^*, v^*)\big) - B(u^*, v^*)C(u^*, v^*) > 0.$$

However, $-T_0(d_2) < 0$, $D_0(d_2) > 0$. Thus, only a pair of eigenvalues have positive real parts, while the others have negative real parts. So E^* is linearly unstable with $d_2 > 0$. For $A(u^*, v^*)+D(u^*, v^*) = 0, T_0 = 0, D_0 > 0$, then (9) owns a pair of purely imaginary roots, and Hopf bifurcation generates.

(ii) The condition means that $-T_k(d_2) > 0$, $k \geqslant 0$. So $-T_k(d_k) > 0$, $D_k(d_k) = 0$. From the assumption $d_{2k_1} \neq d_{2k_2}$, $k_1 \neq k_2$, $1 \leqslant k_1, k_2 \leqslant k_0$, it is easy to see that $D_k(k_1) \neq 0$, $k_1, k \geqslant 1$, $k_1 \neq k$. With $k \leqslant k_0$, there exists

$$D'_k(d_{2k}) = \mu_k\big[d_1\mu_k - A(u^*, v^*)\big] \neq 0.$$

Therefore, (d_{2k}, E^*) is the steady state bifurcation point for the fixed $1 \leqslant k \leqslant k_0$.

(iii) The existence is similar to (ii), and the details are omitted. The second part will be verified. In fact, for $d_2 < \overline{d}_2$, $k \geqslant 1$, we have $D_k(d_2) > 0$, $-T_k(d_2) > 0$. Moreover, $D_0(d_2) > 0$, $-T_0(d_2) < 0$, which imply that the conclusion is valid.

(iv) The existence is omitted. By the assumption we have $T_1(d_{21}^H) = 0$, $T_k(d_{21}^H) \neq 0$, $k \geqslant 0$, and $-T_0(d_{20}) < 0$. In addition, $D_0(d_{20}) \neq 0$ for all $d_{20} > 0$. Clearly,

$$\begin{aligned} D_1(d_{21}^H) &= \big[d_1\mu_1 - A(u^*, v^*)\big]\big[A(u^*, v^*) - d_1\mu_1\big] - B(u^*, v^*)C(u^*, v^*) \\ &= -d_1^2\mu_1^2 + 2d_1\mu_1 A(u^*, v^*) - A(u^*, v^*)^2 - B(u^*, v^*)C(u^*, v^*). \end{aligned}$$

Obviously, if condition (31) holds, then $D_1(d_{21}^H) > 0$. Moreover, if $\mu_1 > (A(u^*, v^*) + D(u^*, v^*))/2d_1$, then $\mathrm{d}D_k/\mathrm{d}\mu_k > 0$. Thus, $D_k(d_{21}^H) \geqslant D_1(d_{21}^H) > 0$. Therefore, Eq. (9) has conjugate complex eigenvalues

$$\lambda = \frac{1}{2}\big\{T_1(d_2) \pm \mathrm{i}\sqrt{T_1^2(d_2) - 4D_1^2(d_2)}\big\}.$$

Clearly, $\mathrm{Re}'(\lambda) = \mu_1/2 \neq 0$.

As a result, (d_{21}^H, E^*) is Hopf bifurcation point, which indicates that (2) has a lot of inhomogeneous periodic solutions near E^*. □

Remark 7. In (ii), if there exist μ_i $(i = 1, 2, 3, \ldots)$ such that $0 < k_1 < \mu_i < k_2$, then Turing instability appears, where k_1, k_2 are the roots of $D_k = (d_1\mu_k - A(u^*, v^*))(d_2\mu_k - D(u^*, v^*)) - B(u^*, v^*)C(u^*, v^*) = 0$.

Remark 8. If $d_{2k}^H = d_{2k}^S$, Turing–Hopf bifurcations occur, which means that (2) oscillates both spatially and temporally.

6 Numerical simulations

Finally, we display numerical simulations to exemplify our previous results.

6.1 Effect of the toxin θ_2 and the threshold harvesting T on the essential dynamics

Fix $r = 0.7$, $h = 0.06$, $f = 1$, $\eta = 0.05$, $\theta_1 = 0.9$. Figure 2 manifests that θ_2 affects the number of the equilibria. Figure 3 shows that h can also change the number of positive equilibria. The rise of h cannot make the prey density, and the predator density coexist.

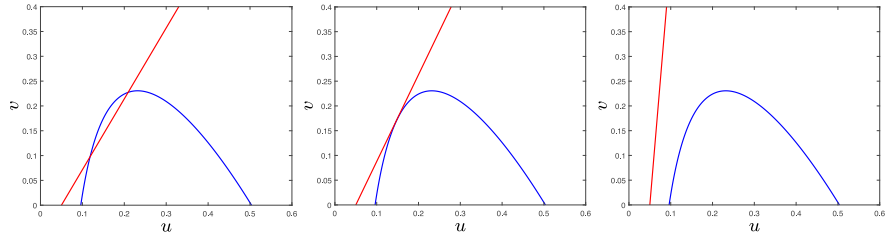

Figure 2. The blue curves are the prey isoclines, and the red lines are the predator isoclines. For $\theta_2 = 0.7$, there are two equilibria. For $\theta_2 = 0.57$, there is one equilibrium. For $\theta_2 = 0.1$, there is no equilibrium.

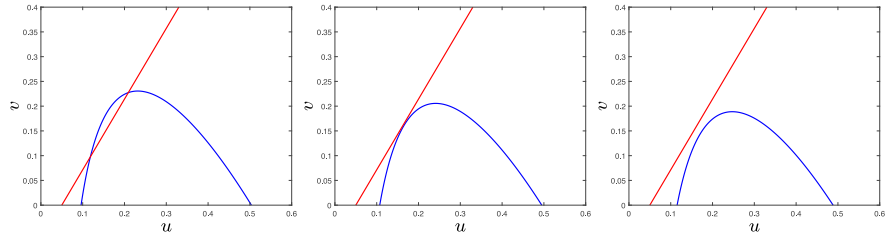

Figure 3. The blue curves are the prey isoclines, and the red lines are the predator isoclines. For $h = 0.06$, there are two equilibria. For $h = 0.0659$, there is one equilibrium. For $h = 0.07$, there is no equilibrium.

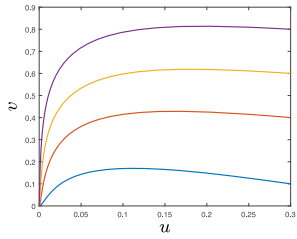

Figure 4. The trivial state steady solution to system (2) is globally asymptotically stable.

Take $r = 0.6$, $T = E = 0.7$, $\theta_1 = 0.25$, $h = 1$, $\theta_2 = 0.2$. So $r - 2rT - 3\theta_1 T^2 = -0.39 < 0$, $rT(1-T) - \theta_1 T^3 = 0.09 < h$, and Fig. 4 is consistent with Theorem 3.

In this subsection, the distinct spatially properties of solutions are obtained by choosing different harvesting threshold T. $r = 0.7$, $\theta_1 = 0.9$, $\eta = 0.05$, $d_1 = 0.008$, $d_2 = 1$, $\Omega = (0, \pi)$. With $T = 0.5$, so $u^* = 0.5085 > T$, and the positive solution is stable as shown in Fig. 5. But it loses its stability owing to inhomogeneous spatial perturbation $u^* = 0.4492 < T$ in Fig. 6. With $T = 0.3$, $\beta_2 = 0.003$, the positive steady state is unstable with $u^* = 0.162 < T$ in Fig. 7, but the positive steady state is locally asymptotically stable with $u^* = 0.33 > T$, $h = 0.003$, $\theta_2 = 0$ in Fig. 8. It can be seen that the presence of the toxin β_2 alters the dynamic behavior of (2). The homogeneous periodic solution of (2) in Fig. 9 can be obtained, which is consistent with Theorem 8.

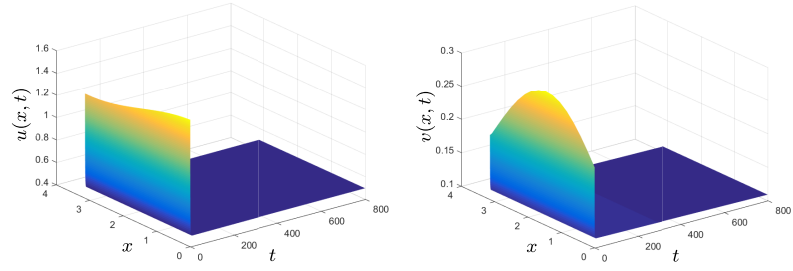

Figure 5. $E^* \approx (0.5085, 0.0917)$ is stable with $T = 0.5$, $u^* = 0.5085 > T$, $h = 0.01$, $\theta_2 = 0.0005$.

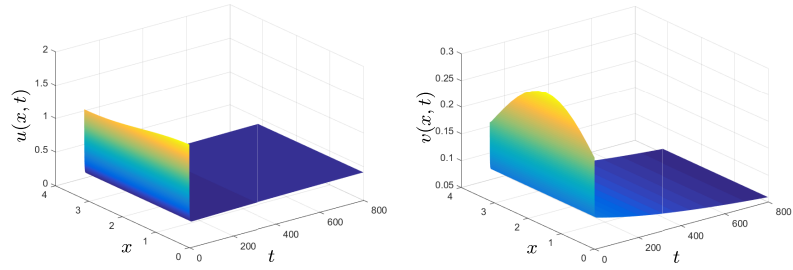

Figure 6. $E^* \approx (0.4492, 0.2316)$ is unstable with $T = 0.5$, $E = 0.2$, $u^* = 0.4492 < T$, $\theta_2 = 0.01$.

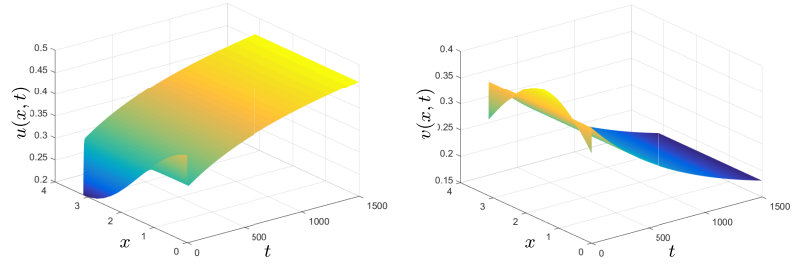

Figure 7. $E^* \approx (0.162, 0.56)$ is unstable with $T = 0.3$, $u^* = 0.162 < T$, $E = 0.003$, $\theta_2 = 0.002$.

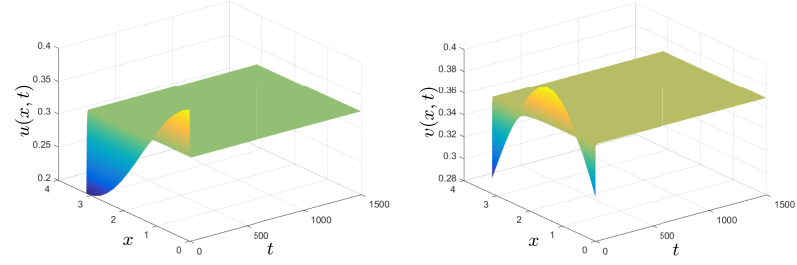

Figure 8. $E^* \approx (0.33, 0.3759)$ is stable with $T = 0.3$, $u^* = 0.33 > T$, $h = 0.003$, $\theta_2 = 0$.

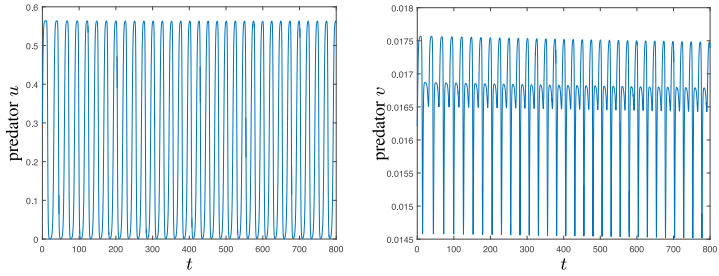

Figure 9. Numerical simulation on the dynamics of the bifurcating periodic solution to system (2) with $\eta = 0.21$, $h = 0.001$, $\theta_2 = 0.00001$, $d_1 = 4$, $d_2 = 0.1$.

6.2 Effect of the toxin θ_2 on the pattern formations

In this subsection, different spatial patterns of the prey are observed by varying θ_2 reflecting the effects of the toxin on the prey. Figure 10 shows the spatial pattern of the prey at $t = 20000$ by choosing $r = 0.7$, $h = 0.001$, $\theta_1 = 0.9$, $c = 1$, $\eta = 0.05$, $d_1 = 0.1$, $d_2 = 6$. When θ_2 is set as 0, that is to say, there is no toxin on the predator, the stationary state pattern is presented. It looks irregular. With the increase of θ_2, it can be seen that the random initial distribution leads to the formation of coexistence of the spotted patterns, the spotted patterns and the fewer spotted patterns, and the stripe-like patterns exist. For

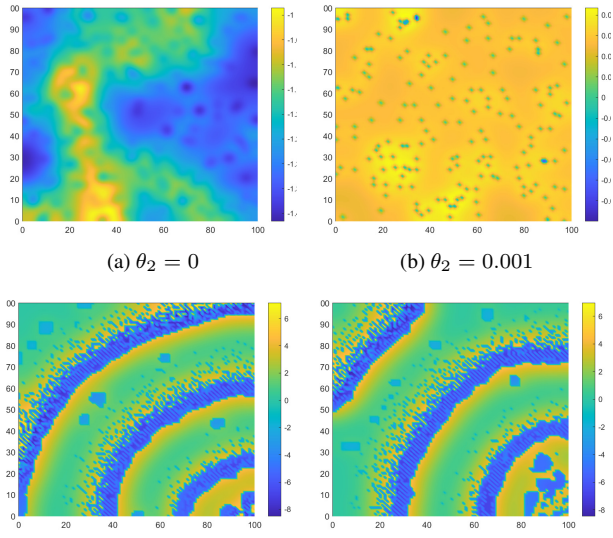

(a) $\theta_2 = 0$ (b) $\theta_2 = 0.001$

(c) $\theta_2 = 0.005$ (d) $\theta_2 = 0.006$

Figure 10. Patterns of the prey density for system (2).

few toxins, the distribution of the prey exhibits spotted patterns, which means that the population is isolated with low density surrounded by high quantity, representing the prey dominance of the spatial domain. Further increase in the toxin results in the disappearance of hole patterns, and only stripe patterns remain present in the domain.

6.3 Effect of the diffusion rate d_2 on the pattern formations

In Fig. 11, fix $r = 0.7$, $h = 0.001$, $\theta_1 = 0.9$, $c = 1$, $\eta = 0.05$, $\theta_2 = 0.005$, $d_1 = 0.1$. There are patterns by varying d_2. It shows a transformation from labyrinth patterns to spot patterns with intermediate states stripe patterns and mixed patterns. As $d_2 = 0.17$, the labyrinth patterns will dominate. When $d_2 = 0.2$, the spot and stripe patterns exist. As d_2 grows to 0.4, the labyrinth patterns occur. With further increase of d_2, only stripe patterns

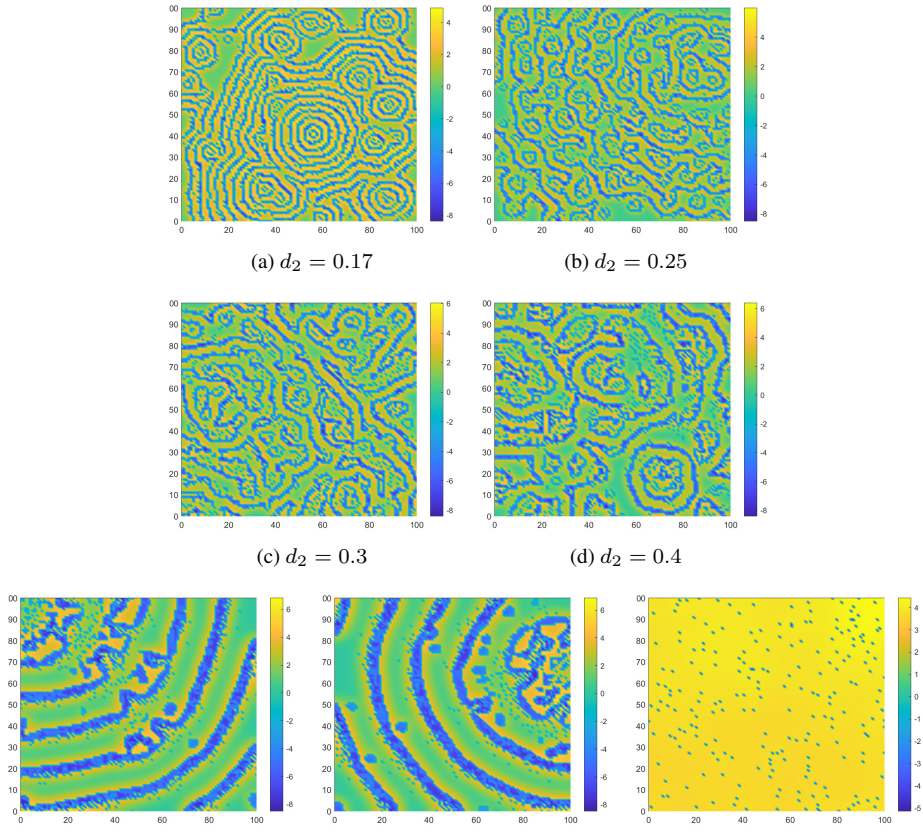

(a) $d_2 = 0.17$ (b) $d_2 = 0.25$

(c) $d_2 = 0.3$ (d) $d_2 = 0.4$

(e) $d_2 = 1.5$ (f) $d_2 = 1.7$ (g) $d_2 = 5$

Figure 11. Patterns of the prey density for system (2) at time $t = 20000$.

occur. When d_2 becomes larger, mixed patterns appear. At last, we set d_2 as 5, and the spot patterns arise. For intermediate values of d_2, the formation of the labyrinth patterns are prevalent. With the high diffusion rate, a mixture of stripe and hole patterns emerges, and a high-density prey gradually masters the regions. The values of d_2 can affect the cohabitation of them.

7 Conclusion

In the article, the dynamics of a predator–prey system containing toxic substances and the threshold harvesting are studied. We have established sufficient conditions for the permanence of (2), implying that both densities exist together. The stabilities of some nonnegative solutions are analyzed. Some sufficient conditions for some special solutions are also established. Meanwhile, we have studied Turing patterns and the bifurcation analysis.

We deliberate pattern dynamics of the system via the multiple scale analysis. By simulation results we find that the different patterns are due to d_2 and θ_2. The patterns can explain the prey and predator distribution in reality, and the dynamic complexity during the ecological environment.

There will be some questions: other environmental factors such as seasonal changes are not considered in our paper. We leave these open issues for future investigation.

References

1. A.D. Bazykin, *Nonlinear Dynamics of Interacting Populations*, World Scientific, Singapore, 1998.
2. S.J. Chan, J. Labadin, Y. Podin, A dynamic seipr model for the spread of hand, foot and mouth disease in sarawak, *Journal of Telecommun. Electron. Comput. Eng.*, **9**(3–10):125–129, 2017.
3. A. Das, G.P. Samanta, Modelling the fear effect in a two-species predator–prey system under the influence of toxic substances, *Rend. Circ. Mat. Palermo (2)*, **70**(3):1501–1526, 2021, https://doi.org/10.1007/s12215-020-00570-x.
4. T. Das, R.N. Mukherjee, Harvesting of a prey-predator fishery in the presence of toxicity, *Appl. Math. Model.*, **33**(5):2282–2292, 2009, https://doi.org/10.1016/j.apm.2008.06.008.
5. P. De Mottoni, F. Rothe, Convergence to homogeneous equilibrium state for generalized Volterra–Lotka systems with diffusion, *SIAM J. Appl. Math.*, **37**(3):648–663, 1979, https://doi.org/10.1137/0137048.
6. S. He, S.Y. Tang, Y. Xiao, R.A. Cheke, Stochastic modeling of air pollution impacts on respiratory infection risk, *Bull. Math. Biol.*, **80**(12):503–513, 2018, https://doi.org/10.1007/s11538-018-0512-5.
7. J. Huang, Y. Gong, S. Ruan, Bifurcation analysis in a predator-prey model with constant-yield predator harvesting, *Discrete Contin. Dyn. Syst., Ser. B*, **18**(8):2101–2121, 2013, https://doi.org/10.3934/dcdsb.2013.18.2101.

8. D. Jana, P. Dolai, A.K. Pal, G.P. Samanta, On the stability and Hopf-bifurcation of a multi-delayed competitive population system affected by toxic substances with imprecise biological parameters, *Model. Earth Syst. Environ.*, **2**(3):1–16, 2016, https://doi.org/10.1007/s40808-016-0156-0.
9. J.Huang, S. Liu, S. Ruan, X. Zhang, Bogdanov-Takens bifurcation of codimension 3 in a predator-prey model with constant-yield predator harvesting, *Commun. Pure Appl. Anal.*, **15**(3):1041–1055, 2016, https://doi.org/10.3934/cpaa.2016.15.1041.
10. L. Ji, C. Wu, Qualitative analysis of a predator–prey model with constant-rate prey harvesting incorporating a prey refuge, *Nonlinear Anal. Real World Appl.*, **11**(4):2285–2295, 2010, https://doi.org/10.1016/j.nonrwa.2009.07.003.
11. T.K. Kar, K.S. Chaudhuri, On non-selective harvesting of two competing fish species in the presence of toxicity, *Ecol. Model.*, **16**(1–2):125–137, 2003, https://doi.org/10.1016/S0304-3800(02)00323-X.
12. H.F. Li, Environmental harm behind the rapid increase of takeaway garbage, *Ecol. Econ.*, **34**(10):10–13, 2018.
13. M. Liu, K. Wang, Persistence and extinction of a single-species population system in a polluted environment with random perturbations and impulsive toxicant input, *Chaos Solitons Fractals*, **45**(12):1541–1550, 2012, https://doi.org/10.1016/j.chaos.2012.08.011.
14. M. Liu, K. Wang, X.-W. Liu, Long term behaviors of stochastic single-species growth models in a polluted environment, *Appl. Math. Modelling*, **35**(2):752–762, 2011, https://doi.org/10.1016/j.apm.2010.07.031.
15. Y. Lou, W.-M. Ni, Diffusion vs. cross-diffusion an elliptic approach, *J. Differ. Equations*, **154**(1):157–190, 1999, 10.1006/jdeq.1998.3559.
16. A. Mondal, A.K. Pal, P. Dolai, G.P. Samanta, A system of two competitive prey species in presence of predator under the influence of toxic substances, *Filomat*, **36**(2):361–385, 2022, https://doi.org/10.2298/FIL2202361M.
17. A.K. Pal, P. Dolai, G.P. Samanta, Dynamics of a delayed competitive system affected by toxic substances with imprecise biological parameters, *Filomat*, **31**(16):5271–5293, 2017, https://doi.org/10.2298/FIL1716271P.
18. D. Pal, G. S. Mahapatra, Effect of toxic substance on delayed competitive allelopathic phytoplankton system with varying parameters through stability and bifurcation analysis, *Chaos Solitons Fractals*, **87**(1):109–124, 2016, https://doi.org/10.1016/j.chaos.2016.03.019.
19. D. Pal, G.P. Samanta, G.S. Mahapatra, Selective harvesting of two competing fish species in the presence of toxicity with time delay, *Appl. Math. Comput.*, **313**(15):74–93, 2017, https://doi.org/10.1016/j.amc.2017.05.069.
20. O.Y. Qi, *Patterns Formation in Reaction Diffusion Systems*, Education Publishing House, Shanghai, 2000 (in Chinese??).
21. J. Rebaza, Dynamics of prey threshold harvesting and refuge, *J. Comput. Math.*, **236**(7):1743–1752, 2012, https://doi.org/10.1016/j.cam.2011.10.005.
22. S. Saha, G.P. Samanta, Dynamics of an epidemic model with impact of toxins, *Physica A*, **527**(1):121152–123456, 2019, https://doi.org/10.1016/j.physa.2019.121152.

23. G.P. Samanta, Analysis of a nonautonomous delayed predator-prey system with a stage structure for the predator in a polluted environment, *International Journal of Mathematics and Mathematical Sciences*, **2010**:891812, 2010, https://doi.org/10.1155/2010/891812.

24. G.P. Samanta, Analysis of a nonautonomous delayed predator-prey system with a stage structure for the predator in a polluted environment, *Int. J. Math. Math. Sci.*, **2010**:891812, 2010, https://doi.org/10.1155/2010/891812.

25. G.P. Samanta, A two-species competitive system under the influence of toxic substances, *Appl. Math. Comput* ., **216**(1):291–299, 2010, https://doi.org/10.1016/j.amc.2010.01.061.

26. G.P. Samanta, Analysis of nonautonomous two species system in a polluted environment, *Math. Slovaca*, **62**(3):567–586, 2012, https://doi.org/10.2478/s12175-012-0031-z.

27. D.M. Thomas, T.W. Snell, A control problem in a polluted environment, *Math. Biosci.*, **133**(2): 139–163, 1996, https://doi.org/10.1016/0025-5564(95)00091-7.

28. C. Walters, V. Christensen, B. Fulton, A.D.M. Smith, R. Hilborn, Predictions from simple predator-prey theory about impacts of harvesting forage fishes, *Ecol. Model.*, **337**(1):272–280, 2016, https://doi.org/10.1016/j.ecolmodel.2016.07.014.

29. J.-S. Wang, Y.-P. Wu, L. Li, G.-Q. Sun, Effect of mobility and predator switching on the dynamical behavior of a predator-prey model, *Chaos Solitons Fractals*, **132**(1):109584–111111, 2020, https://doi.org/10.1016/j.chaos.2019.109584.

30. D. Wu, H. Zhao, Y. Yuan, Complex dynamics of a diffusive predator–prey model with strong Allee effect and threshold harvesting, *J. Math. Anal. Appl.*, **469**(2):982–1014, 2019, https://doi.org/10.1016/j.jmaa.2018.09.047.

31. X. Zhang, H. Zhao, Dynamics and pattern formation of a diffusive predator–prey model in the presence of toxicity, *Nonlinear Dyn.*, **95**(1):2163–2179, 2019, https://doi.org/10.1007/s11071-018-4683-2.